



Optimum anamorphic image generation using image rotation and relative entropy

L. K. Pavithra¹ · R. Srinivasan² · T. Sree Sharmila²

Received: 26 February 2021 / Revised: 5 January 2022 / Accepted: 27 March 2022 /

Published online: 26 April 2022

© The Author(s), under exclusive licence to Springer Science+Business Media, LLC, part of Springer Nature 2022

Abstract

Anamorphosis is related to the art that gives illusion (distortion) over the image or object when the viewer looks the original image or from the random viewpoint. This illusion effect is nullified when the image or object is viewed from the standard viewpoint. In digital imaging domain, anamorphic images (distortion) are generated by changing the pixel coordinates of the given image into new pixel coordinates, and this process typically increases the size of the original image matrix which results in gaps between the successive pixels. In anamorphic transform, the gaps between the successive pixel positions increases as we travel from viewing end to the tail end, and these gaps are filled by interpolating the successive pixels. The viewing angle, distance, height between the viewer and original image are responsible for the amount of distortion introduced in anamorphic images. The proposed work reveals that the rotation of the original image also plays an important role in creating distortion in anamorphic images. The proposed work uses the Kullback-Leibler distance (KLD) to measure the amount of distortion between the original and anamorphized images. A larger KLD implies that the original and anamorphic images are well separated i.e., a good anamorphism has achieved. It is found that the smaller viewing angle combined with the viewing distance and height achieves the larger KLD. The optimum anamorphic image generation is done at two levels: (i) Choosing an appropriate viewing angle, distance, and height, and (ii) Choosing the appropriate rotation of the image to be anamorphized. The former is optimized through KLD, and for the latter Shannon's entropy of the tail portion of the original image under different rotations is used. The proposed technique is tested on various images with different resolutions and is found to be working properly.

Keywords Anamorphic · Relative entropy · Shannon's entropy · Image rotation

✉ L. K. Pavithra
pavithrra.pavi@gmail.com

¹ School of Computer Science and Engineering, Vellore Institute of Technology, Chennai 600127, India

² Department of Information Technology, Sri Sivasubramaniya Nadar College of Engineering, Chennai 603110, India

1 Introduction

Anamorphosis is related to art, and an anamorphic image is a distorted image that looks distorted when viewed directly but undistorted when viewed from correct perspective or in reflection from a curved surface [20]. There are two types of anamorphosis (i) Plane or perspective and (ii) Mirror [17]. In the perspective anamorphosis (planar anamorphosis), from the appropriate perspective point, the intended image can be seen. This technique dates to year AD 1500 [17]. Even though this art is old, it keeps attracting the artists. The mirror anamorphosis distorts an original image, and the original image is got back with the help of appropriate perspective point on the cylindrical or conical mirror [2]. The mathematical models of the planar and mirror anamorphic transformations are given by Hunt et al. [11] and De Weerd et al. [5]. Anamorphic of 3D structures are studied by Hansford and Collins [9]. Anamorphic projection on the complex surface is derived by Di Pola et al. [7]. Topper [21] proposed a new perception over anamorphic images. Moreover, dynamic anamorphic images are acted as the computer user interfaces which gives non-deformed images to user even the user eyes are moving from one place to another [15]. Paolo Di et.al [6] explained the journey of anamorphic images in the field of arts, history, and geometry. Javier and Chacon [16] have obtained the anamorphic deformation of the bitmap image or object by changing the control points in radial direction on the rational Bézier surface but the amount of distortion appeared in the deformation is not considered. Amount of distortion available in the anamorphic image is directly proportional to the predictability of original image involved in anamorphization when it viewed from the undesired viewpoints. Therefore, Vesna Stojakovic and Bojan Tepavcevic [19] have studied the amount of distortion available in the anamorphic images under three cases such as (i) viewing direction (ii) viewing angle and (iii) viewing distance using the Rhinoceros tool. The high distorted anamorphic image is obtained when the viewing direction is parallel to the picture plane combined with the viewing angle less than 10° and viewing distance closer to the image. Bobby Stefy et al. [1] have constructed the planar anamorphic images based on mathematical model given by Hunt. et al. [11] in different viewing angle, height, and distance. The amount of distortion available in the anamorphic images is analyzed by the entropy of that image. Likewise, image distortion study plays an important role in image steganography field because distorted image increases the embedding capacity, invisibility and security of the data used in encryption or data hiding [14, 18].

For distortion analysis, Bobby Stefy et al. [1] have used the Shannon-entropy. Kullback-Leibler divergence, also known as relative entropy, is used in image enhancement [22]. Since this metric is asymmetric, a distance metric using Kullback-Leibler divergence has been proposed [4] and is known as Kullback-Leibler distance (KLD), and this metric is used to measure the deviation between the original and transformed image [10]. As stated previously, the anamorphic transformation changes the image matrix size, i.e., the size of the original and anamorphized images are not same. Also, we can notice from Fig. 1 that the anamorphic image is trapezoid shaped whereas the original image is square shaped. Therefore, resizing of the images will not be useful. Therefore, the proposed work uses KLD to compare the original and anamorphized images which are not of same size and same shape.

1.1 Motivation, contribution and organization

The anamorphic models generate the anamorphic images using viewing angle, height, and distance. The impact of viewing point or rotation is not captured in the existing models. The

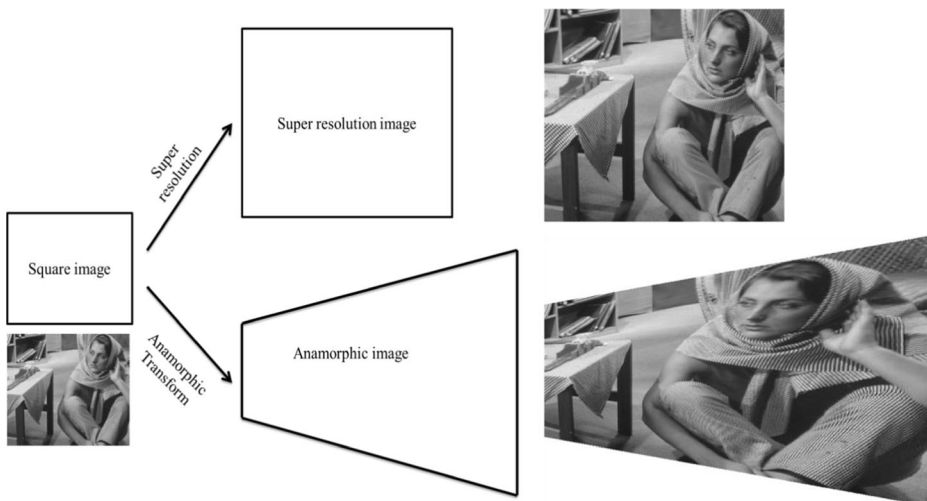


Fig. 1 Resulting image after applying super resolution and anamorphic transform on square shape image

rotation of the original image with respect to the perspective point is an important parameter which is not addressed in the literature to the best of our knowledge. Moreover, the analysis over the generated anamorphic image (i.e., level of distortion) is also not effectively carried out in the literature. It has been observed that there is no optimum anamorphic image generation algorithm available in the existing literature. This motivates us to propose the optimal anamorphic image generation method by analyzing the amount of distortion available in the anamorphized image.

An algorithm to generate optimum anamorphic images has been proposed based on the information theoretic metrics, entropy. By default, any anamorphic scheme must use interpolation techniques. Three different interpolation techniques have been investigated in this paper. The algorithm has been tried on various images to generate optimum anamorphic images, and to evaluate the performance of the proposed algorithm. This work considers the planar anamorphic image for distortion analysis.

The organization of the paper is as follows, section 2 discusses the anamorphic image generation and the interpolation schemes used in the process. Section 3 analyses the effect of viewing angle, distance, and height on anamorphic transform. Section 4 presents a procedure to generate an optimum anamorphic image from the given image. Section 5 shows the importance of image rotation in optimal anamorphic image generation and results are compared with the state-of-the-art techniques. Conclusions are briefed in section 6.

2 Generation of anamorphic images

This section illustrates the procedure involved in 2D plane anamorphic image generation and discusses effects associated with this transformation. In this work, anamorphic image generation and its associated analysis have been explored using MATLAB. Plane anamorphism is the mapping of points (x, y) in a target plane to points (x', y') on the anamorphic plane [11]. This mapping typically increases the size of the original image matrix, and it differs from super resolution in the following two ways: (i) the gaps generated due to super resolution process is

constant throughout the image whereas in anamorphic transform the gaps between the successive pixels positions increase as we travel from viewing end to tail end, and (ii) a rectangular/square image becomes trapezoidal image after applying anamorphic mapping (region 1 in Fig. 1) whereas the super resolution maintains the shape as shown in Fig. 1. The gaps generated during the anamorphic transform must be filled in using interpolation schemes. Anamorphic transformation is captured through three parameters called viewing angle, distance, and height from where the image is viewed [11] (perspective point).

As stated above, anamorphic transformation is mapping of the original image's pixel coordinates (x, y) into new pixel coordinates (x', y') . Even though the anamorphic image is trapezoid shaped, we use rectangular shaped matrix to represent the anamorphic image in order to handle the images in machines, and is shown in Fig. 2. There are three regions in Fig. 2, region 1, region 2 and region 3. Among these, only region 1 has the information about the anamorphic image. The region 2 and region 3 are added to produce a rectangular shaped matrix. With this setup we have two matrices, one in the target plane (original image matrix of size $(m \times n)$, and another in the anamorphic plane (new matrix of size $(M \times N)$). The target and anamorphic planes are orthogonal to each other.

The anamorphic transform maps the $(m \times n)$ matrix elements to the region 1 of the $(M \times N)$ matrix. The region 2 and 3 can be either filled with 0 or 255. Assuming the target plane is normal to the origin of line of sight, x' and y' can be related to x and y using the following expressions [4],

$$y' = \frac{y}{\sin(\alpha)} \cdot \frac{1}{\left[1 - \left(\frac{y}{h}\right) \cos(\alpha)\right]} \quad (1)$$

and

$$x' = \frac{x}{\sqrt{\left[h^2 + d^2 + y^2\right]}} \cdot \sqrt{\left[h^2 + (d + y')^2\right]} \quad (2)$$

where h is the height from the center of the leading edge of the anamorphic image, and d is the distance from the anamorphic image, and α is the viewing angle. The relation between these three parameters is given in Eq. (3).

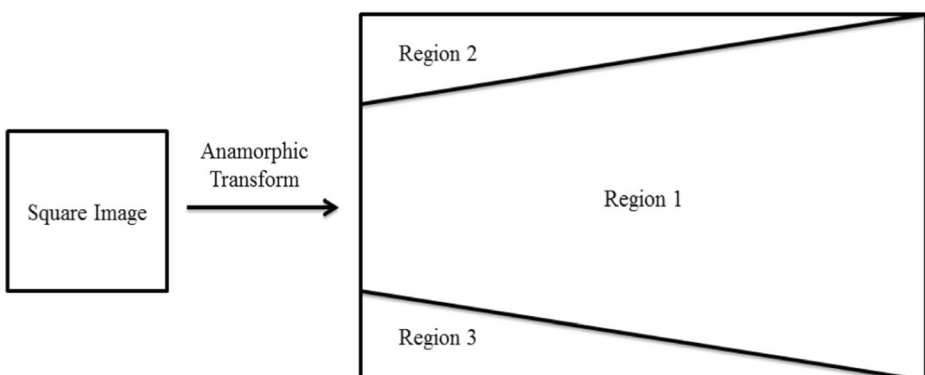


Fig. 2 2D plane anamorphic image generation

$$\tan(\alpha) = \frac{h}{d} \quad (3)$$

To facilitate the understanding of the above parameters Fig. 3 is reproduced from Hunt et al. [11]. The image (of size $m \times n$) to be anamorphized has two ends, viewing end and tail end. x and y directions of the original image are given in Fig. 4. The viewing end y coordinate starts with 1, the first column of the matrix i.e., y is counted from viewing end (starting from 1) to tail end (stopping with n). A particular y is called y_i i.e., i^{th} column is shifted to y'_i using eq. 1. On i^{th} column, we have m number of x values. The y'_i is used to compute m number of x' values corresponding to all x values of y_i i.e., for every y , eq. (1) is used to find out y' , and plugging this y' into eq. (2), x' are calculated for $x = 1$ to m . This process is repeated for all the columns to get the anamorphic image i.e. we compute n number of y' values, $\{y_1', y_2', \dots, y_n'\}$, and $(m \times n)$ number of x' values $\{x_{11}', x_{12}', \dots, x_{1m}', x_{21}', x_{22}', \dots, x_{2m}', \dots, x_{n1}', x_{n2}', \dots, x_{nm}'\}$. The y' corresponding to n^{th} column (N), and the corresponding m^{th} - x' (M) value decide the anamorphic image size ($M \times N$).

For example, if we consider a 50×50 image matrix then we compute y' for $y = 1, 2, 3, \dots, 50$, and the corresponding y' versus y sketch is given in Fig. 5(a), with h, d, and α is set to 48, 40, and 50 respectively. $y = 1$ is mapped onto $y' = 1$, $y = 25$ is mapped onto $y' = 50$, and $y = 50$ is mapped onto $y' = 200$. We can extract the gaps using the following expression:

$$y'_{(i+1)} - y'_{(i)}, \text{ for } i = 1 : (n-1) \quad (4)$$

Figure 5(b) gives the gaps corresponding Fig. 5(a). Figure 6 (a-d) complete setup of the anamorphic transformation using an example (50×50 image with all the matrix elements set

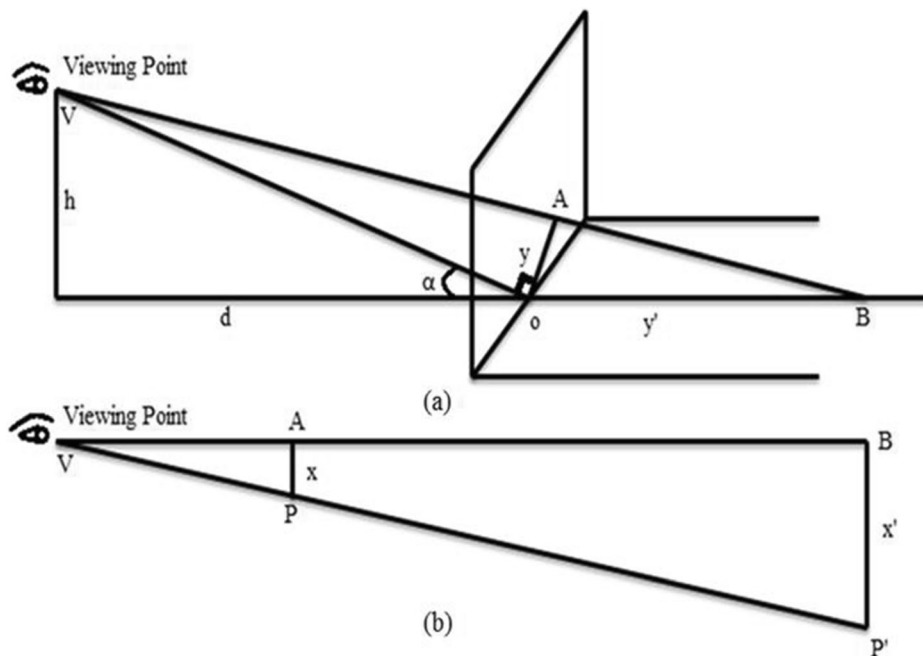


Fig. 3 Geometrical view of anamorphic plane mapping (a) y' (b) x' from original y and x

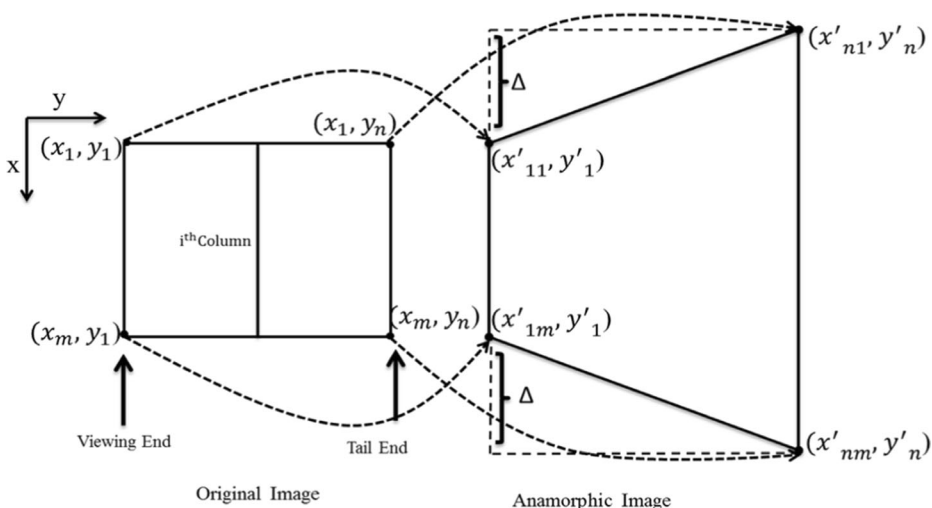


Fig. 4 Mapping from original image pixel location (x,y) to anamorphic image pixel location (x',y')

to a gray value of 128, for h , d , and α set to 48, 40, and 50, respectively). Figure 6(b) depicts the uninterpolated anamorphic image and the non-uniform gaps generated during the anamorphic transformation is clearly visible in Fig. 6(b). The quantified distributions of the gaps are shown in Fig. 6(c).

Figure 6(d) depicts the interpolated anamorphic image. Therefore, the anamorphic process happens in three steps, (i) For each and every position of the original image matrix (x,y) , a new position (x', y') is calculated using eqs. (1) and (2), (ii) The elements from the position (x,y) of the original image matrix is mapped onto (x', y') of the anamorphic image matrix, and (iii) The gaps in the anamorphic image matrix are filled in using interpolation. These steps are shown as a block diagram in Fig. 7. While mapping the elements of $(m \times n)$ on $(M \times N)$ matrix using eqs. (1–2), h , d , and α parameters play an important role. Out of these three parameters, any two can become independent and the remaining becomes a dependent parameter (refer eq. (3)).

The size of the anamorphic image matrix, $(M \times N)$ is decided by h , d , α , and $(m \times n)$. For example, (512×512) matrix changes into $(4312 \times 12,606)$, for $h = 546$ pixels, $d = 1500$ pixels, and $\alpha = 20^\circ$. In the above example, we have 262,144 entries in the $(m \times n)$ matrix, and

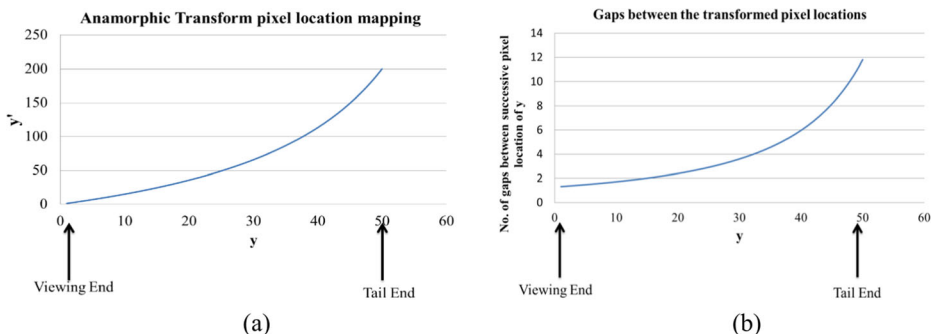


Fig. 5 Relation between original and transformed pixel location mapping

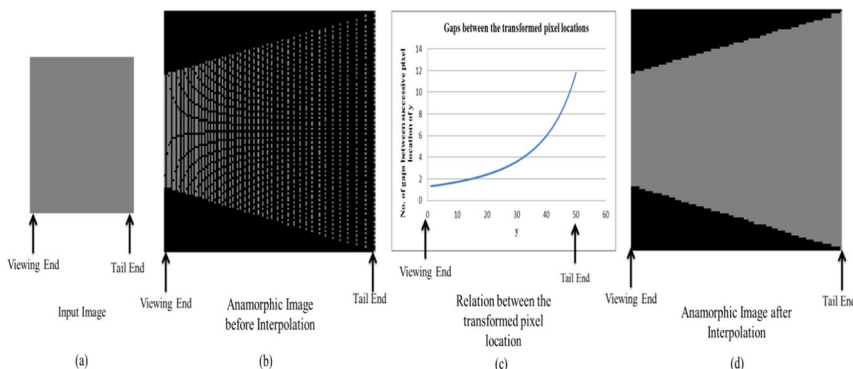


Fig. 6 Anamorphic transformation ($h = 48$, $\alpha = 40$ and $d = 50$) (a) 50×50 square image matrix (b) Anamorphic transform before interpolation (c) Relation between transformed pixel location (d) Anamorphic transform after interpolation

54,357,072 entries ($M \times N$) matrix. Table 1 shows $(M \times N)$ for various h , d and α combinations, for the given $(m \times n)$. Two observations can be made from Table 1 are: (i) For the given α working with larger h and d decreases $(M \times N)$, and (ii) As α increases $(M \times N)$ decreases. These two observations lead to the following conclusion, smaller the h , d , and α bigger the anamorphic image.

As stated in section 2, even though the anamorphic image is trapezoid shaped, a rectangular shaped matrix is used to represent the anamorphic image to handle the images in machines. There are three regions in the $(M \times N)$ matrix, region 1, region 2 and region 3. Among these, only region 1 has the information about the anamorphic image, and the total number of elements of the anamorphic image should come only from region 1. While the number of elements in the original image matrix can be calculated as $(m \cdot n)$, the number of elements in the anamorphic image cannot be given as $(M \cdot N)$. Hence, we need to calculate the number of elements in the region 1 alone (refer Fig. 8). The region 2 and region 3 are triangular shaped, and the number of elements in each of these regions can be given by,

$$\text{Number of elements in region 2 or region 3} = \frac{1}{2} \cdot \Delta \cdot N \quad (5)$$

$$\Delta = (x'_{n1} - x'_{11}) = (x'_{1m} - x'_{nm}) \quad (\text{where})$$

The number of elements in the region 1 of the $(M \times N)$ matrix can be computed as below,

$$\text{Number of elements in region 1} = M \cdot N - 2 \left(\frac{1}{2} \cdot \Delta \cdot N \right) \quad (6)$$

The last column of the Table 1 gives the total number of elements (calculated using eq. (5) to (6)) of the anamorphized image, for various combinations of h , d , and α . Fig. 9 depicts the total number of elements (i.e., $M \cdot N$) of the anamorphic image matrix (calculated using Eq. (4)) versus α , for the given $d (=1500)$. But, h , d , and α

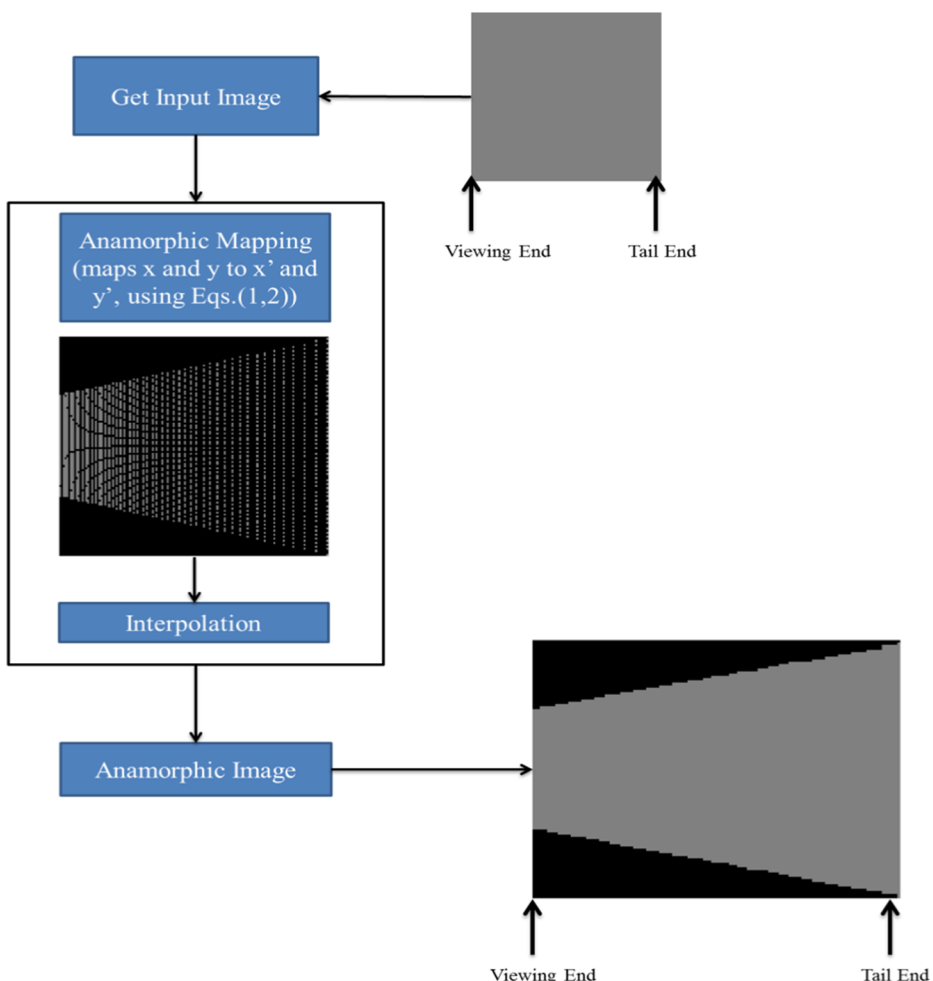


Fig. 7 Block diagram of anamorphic image generation system

Table 1 Change in original image matrix (512×512) after applying anamorphic transform, for various h, d, and α combinations

S. No.	(m x n)	A	d	H	(M x N)	Total no. of elements present region1 is calculated using Eq. (6)
1	(512 x 512)	20°	1500	546	$4312 \times 12,$ 606	30,211,393
2		20°	3000	1092	915×2676	1,910,664
3		30°	1500	866	1049×2096	1,635,822
4		30°	3000	1732	688×1376	825,600
5		40°	1500	1259	744×1157	726,596
6		40°	3000	2518	606×944	527,931

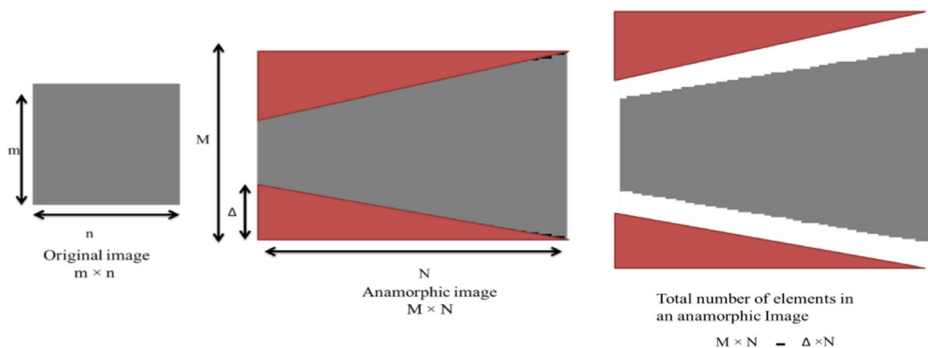


Fig. 8 Calculation of number of elements in region 1

are related to each other as per Eq. (3). If d is fixed, then the change in α should be compensated by the change in h i.e., when α increases h should increase. The lower X-axis of the Fig. 9 shows the α values and the upper X-axis depicts the corresponding h values while d is maintained at 1500.

The anamorphic transform of the (512×512) grayscale Lady image is shown in Fig. 10 after interpolation, for h , d , and α are equal to 1259, 1500, and 40 respectively.

To fill in the gaps generated during the anamorphic transformation, three different interpolations schemes, sample and hold, nearest neighbour, and linear interpolations [8, 12] are used in this study. Figure 11 illustrates the results of anamorphic transformation on the Lady (512×512) image, for three different interpolation schemes. We can see the patch effect is minimized in linear interpolation compared to the other two interpolations.

Table 2 shows the anamorphic images of Lady (512×512) for various combinations h , d and α along with the new resolutions i.e. $(M \times N)$. As already stated, we can observe from Table 2 that lower α , h and d values result in bigger matrices. As stated in the introduction, the square Lady image has become trapezoidal image, and this change in the shape is clearly visible at lower α . When $\alpha = 90^\circ$ the line of sight is normal to the original image, and anamorphic transform does not change the

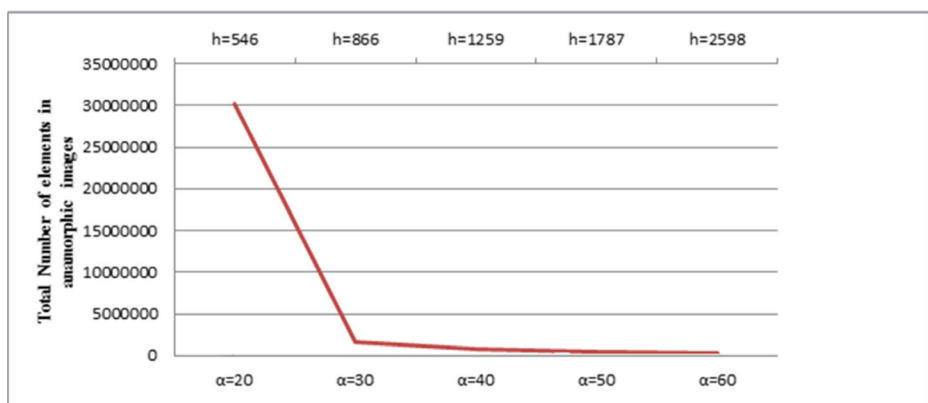


Fig. 9 Total number of elements in the different sized anamorphic images created from the 512×512 image matrix ($d = 1500$)

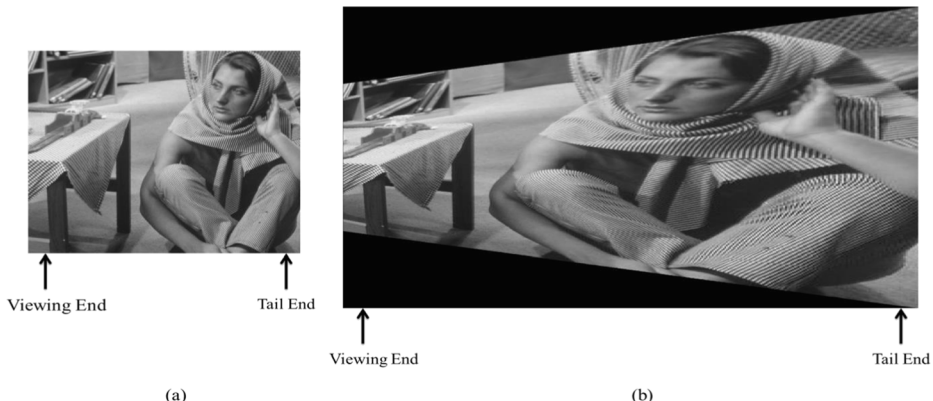


Fig. 10 Anamorphic transform (a) Original image (512×512) (b) Anamorphic image (744×1157)

original image. In other words, it is more difficult to recognize the anamorphic image generated with lower α compared to the anamorphic image generated with higher α . For example, looking at the images with $\alpha = 20^\circ$ and 60° in Table 2, one can see the original Lady image easily in the $\alpha = 60^\circ$ case.

3 Analysis on anamorphic images

The anamorphic image generation from the original image has been explained in the previous section. Qualitatively, it was concluded that not all h , d and α combinations result in the same anamorphic distortion. Specifically, lower h , d and α combination leads to better anamorphic distortion visually (1st entry of the Table 2). This section quantifies the amount of distortion using Kullback-Leibler distance. The amount of distortion available between the original and the distorted image can be evaluated by

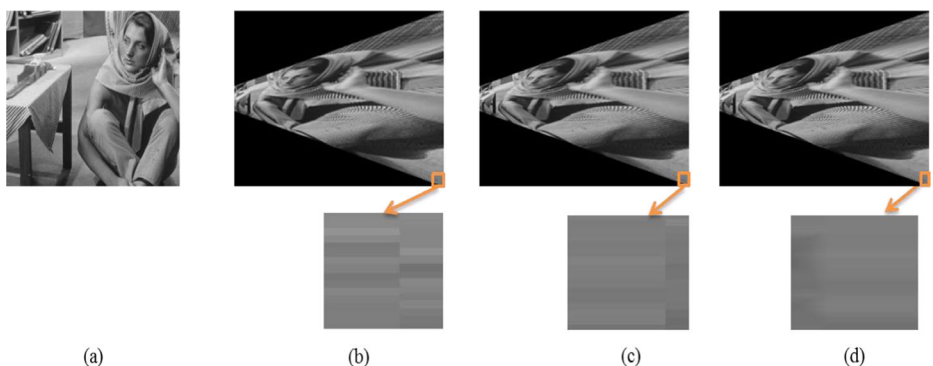
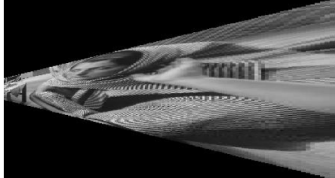


Fig. 11 Output of the interpolation techniques used in anamorphic image generation (a) Original Image (b) Sample and hold interpolation (c) Nearest neighbor interpolation (d) Linear interpolation

Table 2 Anamorphic images of Lady (512×512) at different h , d and α using linear interpolation

Sl. No	α	d	h	Anamorphic Image	(M x N)/resolution after anamorphic transformation
1	20	1500	546		4312×12606
2	30	1750	1010		912×1825
3	40	2000	1678		668×1039
4	50	2500	2979		576×751
5	60	2750	4763		625×541

Peak Signal to Noise Ratio (PSNR), Structural Similarity Index Measure (SSIM), Mean Square Error (MSE), and histogram-based metrics. Among these, PSNR, SSIM and MSE demand same matrix sizes i.e., matrix dimensions before and after distortion. But, the anamorphization process increases the size of the original image. Therefore, PSNR, SSIM, and MSE are not suitable for analyzing distortion in anamorphic images. Hence, we have used histogram-based metrics. This is done by

comparing the histograms of the original and anamorphically distorted images. The normalized histograms can be thought of representing the probability distribution function (PDF) of the image. Therefore, the comparison of the original and anamorphic images is handled as computing the distance between the two PDF i.e., the distance between original image's PDF and the anamorphic image's PDF. For this purpose, the relative entropy or Kullback-Leibler divergence [22] can be chosen which is given by,

$$\text{Kullback-Leibler divergence} = \sum_{i=0}^{255} p_i \log \frac{p_i}{q_i} \quad (7)$$

where p and q are the PDF of the original and anamorphic images. Since there are 256 Gy levels, the index i runs from 0 to 255, and p_i is the probability associated with a particular gray level which can be computed from the image histogram. q_i is the probability associated with the anamorphic image. Kullback-Leibler divergence does not provide symmetric results. With the following definition, Kullback-Leibler divergence becomes Kullback-Leibler distance metric (KLD) [22].

$$\text{Kullback-Leibler distance (KLD)} = \sqrt{\left(\left[\sum_{i=0}^{255} p_i \log \frac{p_i}{q_i} \right]^2 + \left[\sum_{i=0}^{255} q_i \log \frac{q_i}{p_i} \right]^2 \right)} \quad (8)$$

For the given image, anamorphic images are generated with various h , d and α combinations, and the expression (8) is used to calculate the distance between the original and anamorphic images. For example, the KLD values of the first and last entries of the Table 2 are 236.46×10^{-3} and 13.2014×10^{-3} , respectively. This means that the first entry of the Table 2 has a larger anamorphic distortion compared to the last entry of the Table 2. Visually also one comes to the same conclusion. Moreover, the KLD value can be thought of as the original and the anamorphic images are separated very well. The h , d and α combination which offers larger KLD values can be chosen for anamorphization. The pixels from regions 2 and 3 should be removed before going for histogram of the anamorphic image which is done through expressions (5) to (6).

3.1 Impact of different interpolation schemes on the KLD of the anamorphic images

Figure 12 shows the KLD of the anamorphic image (512×512 -Lady image) as a function of α , for three different interpolation schemes namely sample and hold (SH), nearest neighbor (NN), and linear interpolations. The KLD versus α trends are same and their values are also very close, for all the three interpolation schemes. Hence in the rest of the paper, we have used linear interpolation.

3.2 Effect of α , d and h on the KLD of the anamorphic images

Next, the effect of α , d and h on KLD is explored. Eq. (3) tells us that the same α can be obtained for various combinations of d and h . Figure 13 depicts the constant α contours, where the x and y axes are d and h , respectively. For all the combinations of d and h , with $d = \{1500,$

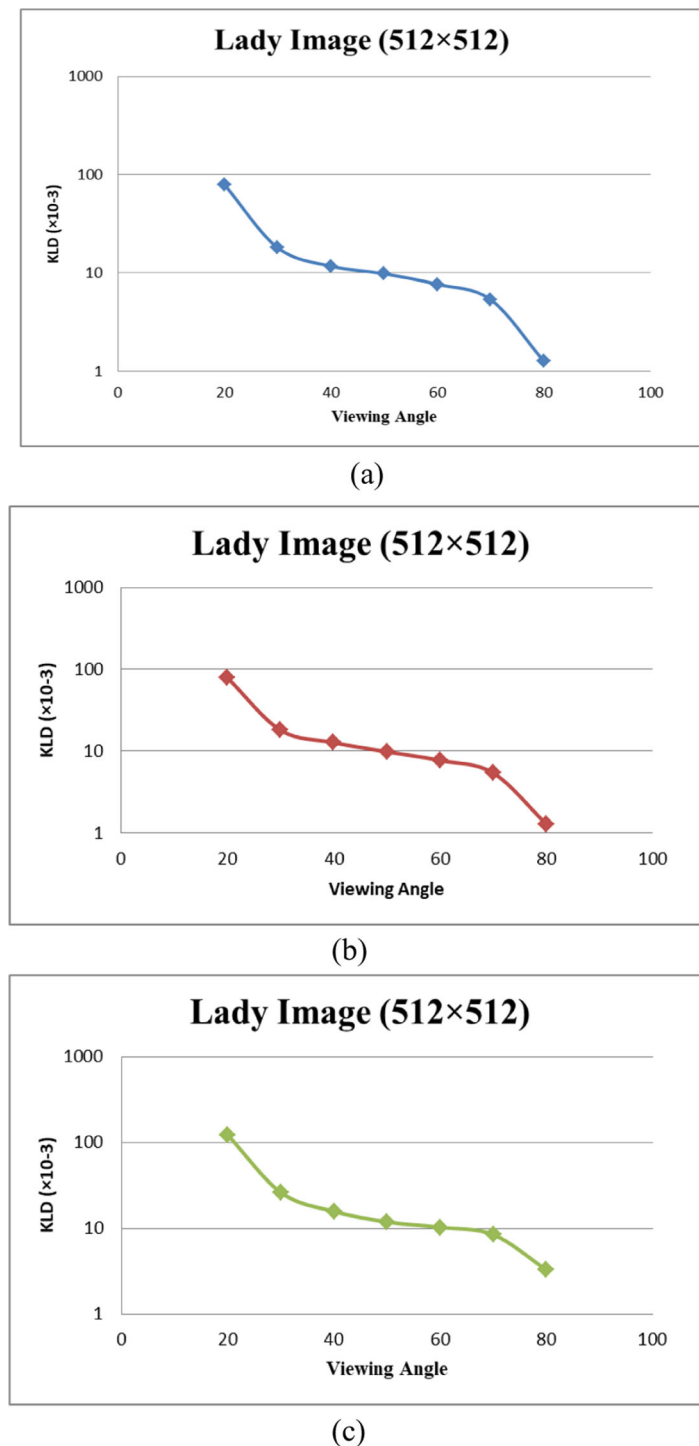


Fig. 12 KLD of (a) Sample and Hold (SH), (b) Nearest Neighbor (NN), (c) linear interpolation techniques used in Lady anamorphic image generation

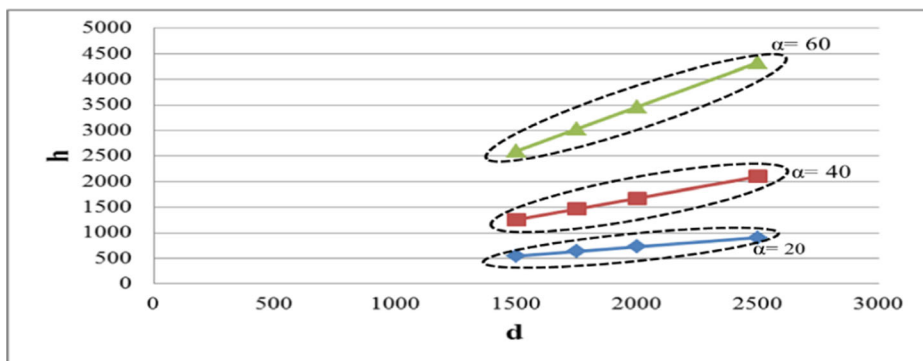


Fig. 13 Constant α contours

1750, 2000, 2500}, and $\alpha = \{20, 30, 40, 50, 60, 70, 80\}$, the corresponding h values are tabulated in Table 3.

Figure 14 shows the KLD as a function of α and h for various d values. For lady image (512×512) the following observations can be made from Fig. 14: (i) As α decreases the KLD increases for the given d , (ii) As d decreases KLD increases for the given α , and (iii) Small α and d values automatically implies small h . Combining the above observations, we can conclude that lower α , d and h offer larger distance between the original and anamorphic images, and maximum distortion is achieved. In other words, an image distorted with lower α , lower d , and lower h is difficult to recognize. Figure 15 (a-c) depicts this scenario where one can easily recognize the Fig. 15(c) but not the Fig. 15 (a) which has lower α , lower d , and lower h .

4 Effect of rotation or viewing end and optimal anamorphic image generation

In the previous section, the anamorphic images were analyzed, for various h , d and α values. Apart from these, the viewing end also plays an important role in anamorphic

Table 3 Different α , d and h combinations used in this experiment to anamorphize the given Lady (512×512) image

$\alpha \rightarrow$ $d \downarrow$	20	30	40	50	60	70	80
1500	546	866	1259	1788	2598	4121	8507
1750	637	1010	1468	2086	3031	4808	9925
2000	728	1155	1678	2384	3464	5495	11,343
2500	909	1443	2098	2979	4330	6869	14,178

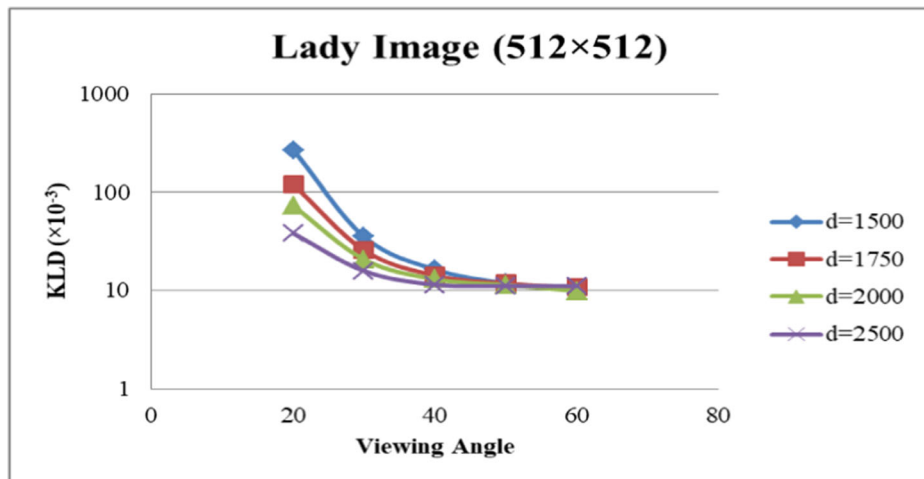


Fig. 14 Anamorphic images KLD analyses based on distance 1500, 1750, 2000, 2500 over target Lady image

distortion. As stated in the introduction section, this has been ignored in the literature. While applying the anamorphic transform the viewing end of the image can be changed by rotating the original image. The rotation changes the viewing end of the image and produces different anamorphic images for different rotations. The optimum rotation is different for different images.

4.1 Brute force method

We can find out the optimum rotation for the effective anamorphic distortion using brute force method. The given image is rotated before applying anamorphic transformation, and this

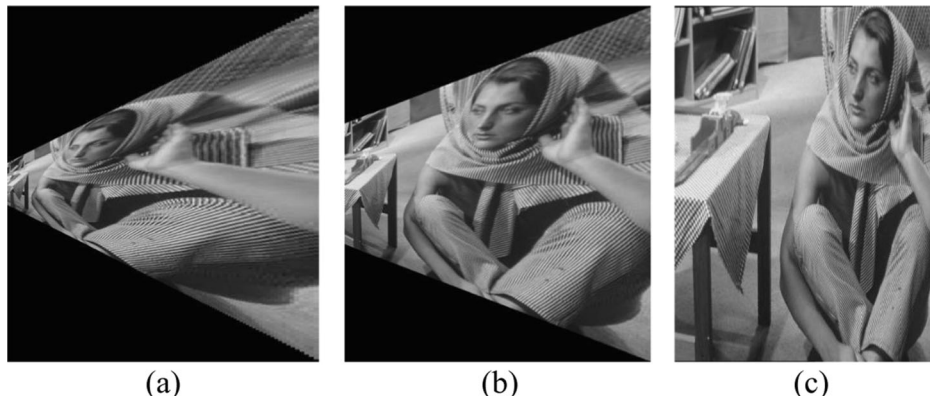


Fig. 15 Anamorphic image with different combination of α , d and h (a) $\alpha = 20$, $h = 546$ and $d = 1500$ (b) $\alpha = 20$, $h = 728$ and $d = 2000$ (c) $\alpha = 80$, $h = 14,178$ and $d = 2500$

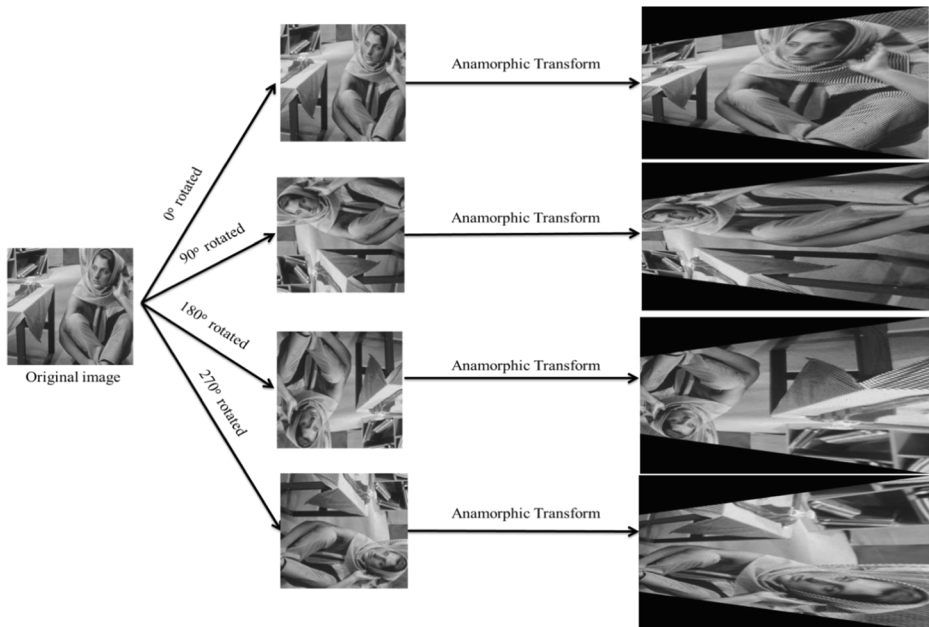


Fig. 16 Anamorphic image of 0° , 90° , 180° and 270° rotated original Lady (512×512) image

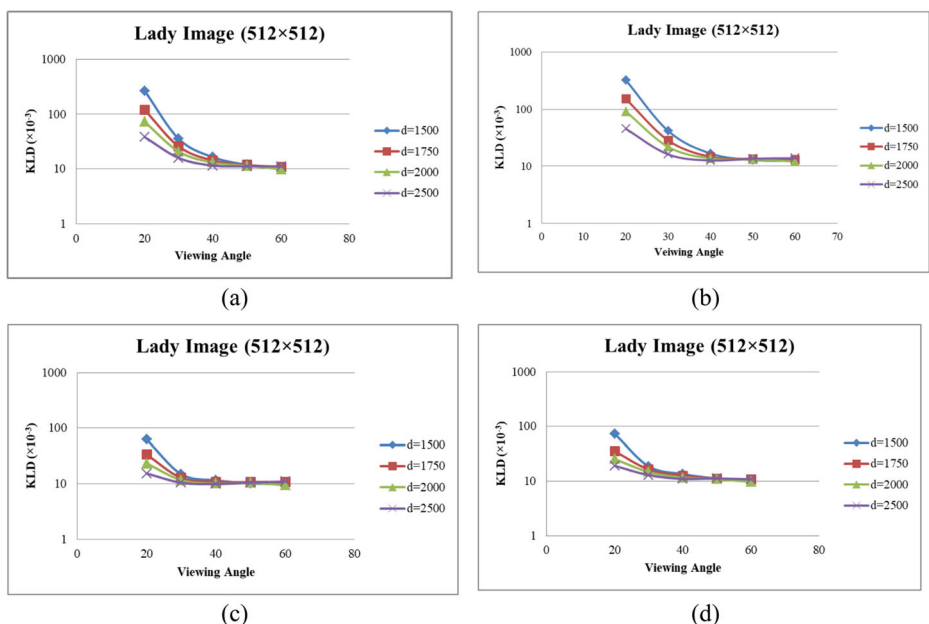


Fig. 17 KLD as a function of α , for four different rotations (a) 0° (b) 90° (c) 180° and (d) 270°

changes the viewing end (Fig. 16). We apply the anamorphic transformation on these rotated images, and then we measure the anamorphic distortions using KLD. The rotation which offers the highest KLD is chosen.

4.2 Optimal rotation or viewing point

The aim is to maximize the distortion. Since different rotations or viewing points offer different number of distortions, the rotation which offers maximum anamorphic distortion is sought using the optimal anamorphic generation algorithm. We can use the results of Fig. 5 (b) which informs us that the successive gaps increase non-linearly as we move from the viewing end to tail end i.e., the tail end goes through more distortion compared to the viewing end. Different parts of the image carry different amount of information, and can be measured using Shannon's entropy [3],

$$H = - \sum_{i=0}^{255} p_i \log(p_i) \Big|_g \quad (9)$$

where p_i is the probability associated with the original image's gray levels. Since the tail end goes through more distortion, the entropy closer to the tail end is more important compared to the viewing end. Low entropy implies small number of edges, and the interpolation process further reduces the number of edges. A low entropy region put at the tail end will smudge the image effectively. The subscript g in eq. (9) refers to the portion of the image on which the eq. (9) is applied. For example, with $g = \frac{n}{2}$, half the portion of the image starting from tail end is considered for entropy calculation. In this paper, we use $g = \frac{n}{6}$ i.e., $(\frac{1}{6})^{th}$ portion of the image is considered for entropy calculation. The original image is made to undergo four different rotations, 0° , 90° , 180° and 270° , and every time the entropy of the $(\frac{1}{6})^{th}$ portion of the image from the viewing end is calculated ($H_{1/6}$) the one with the lowest $H_{1/6}$ is chosen for the tail end. An algorithm to find out the optimum rotation is given below where in we extract entropy information from the $(\frac{1}{6})^{th}$ portion from the tail end.

Algorithm 1: Optimum anamorphic Image Generation

Input: Image of size $(m \times n)$ to anamorphize
Output: Optimum rotation to anamorphize the input image

1. Get the input image (I) of size $(m \times n)$ (to be anamorphized)
 2. Perform the rotation (R) on the input image with R coming from the set $\{0^\circ, 90^\circ, 180^\circ, 270^\circ\}$ resulting in images R1, R2, R3 and R4
 3. Get the $(\frac{1}{6})^{th}$ regions from the tail ends of R1, R2, R3 and R4 and call them T1, T2, T3 and T4
 4. Calculate the entropy [17] of T1, T2, T3, and T4 using Eq. (9) and call them E1, E2, E3, and E4.
 5. Choose the minimum from {E1, E2, E3, E4} and select the corresponding rotation as the optimum rotation
-

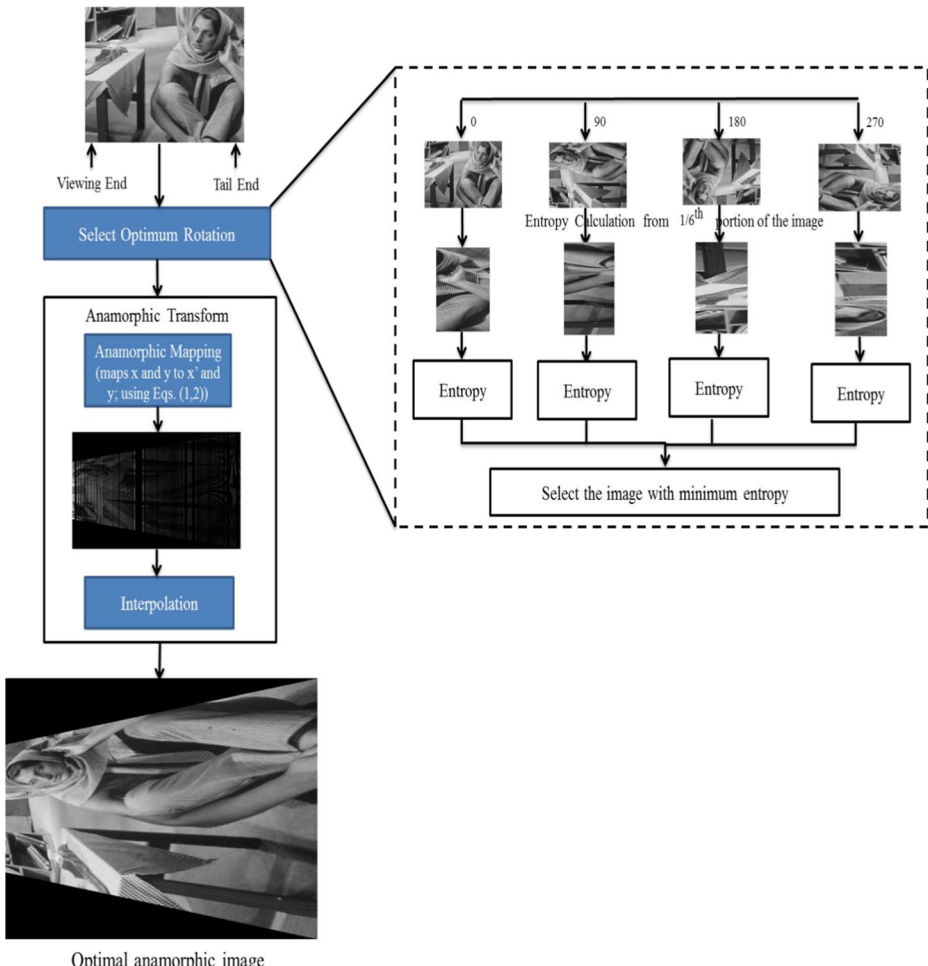


Fig. 18 Block diagram of optimum anamorphic image generation system

5 Experimental results and discussions

The anamorphic transform results in trapezoidal image; the rotation becomes an important parameter i.e. the anamorphic transform applied on the same image but having different orientations will produce different anamorphic images (refer Fig. 16). The rotation changes the viewing end of the image and produces different anamorphic images for different rotations. This implies that the KLD of the two anamorphic images with the same α , d and h values but with different rotations need not be same. Figure 17 (a)-(d) show KLD versus α , for 0°, 90°, 180° and 270° rotations

respectively, for (512×512) lady image. The highest KLD is obtained at 90° rotation, and the lowest KLD at 180° (refer Fig. 17 (d) and (c)) i.e., 90° rotation effectively distorts the image, and can be called as optimum rotation which achieves effective anamorphic distortion.

Figure 18 depicts the block diagram of the optimum anamorphic generation. After getting the original image, the optimum rotation for anamorphic transform is found out as using algorithm 1. Then with the given α , d and h values, the anamorphic distortion is obtained using eqs. (1) and (2) which is followed by the interpolation. If we have the freedom of choice on α , d and h then low α , d and h values are to be chosen as discussed in section 3.2.

The proposed optimal anamorphic generation algorithm is applied over the standard test images [18], 10 different categories of 1000 images present in the Wang's database [13]. Table 4 shows the result for the proposed work on the standard test images (Sl.No: 1,2,3,4,5,8,10), random images taken from internet (Sl.No:6,7,9,11) and a sample image from 10 different categories of images available in Wang's database [13] (Sl.No: 12–21). It can be noticed from Table 4 that the image with different resolutions is chosen, and this is done to validate the proposed algorithm's robustness. Entropy for four different

Table 4 Optimal rotation selection for anamorphic image generation

SL.No	Input Image (m×n)	Entropy of the $\frac{1}{6}$ portion of the original image for different rotations				KLD between original and anamorphic images for different rotations $\alpha=20$, $d=1500$ and $h=546$			
		0°	90°	180°	270°	0°	90°	180°	270°
1	 (512×512)	5.893	6.420	3.161	1.326	205.75	581.614	579.47	1086
2	 (512×512)	7.423	7.199	7.125	6.490	89.65	223.23	305.66	379.13
3	 (512×512)	7.051	6.970	7.240	7.413	181.8	309.91	119.13	132.62

Table 4 (continued)

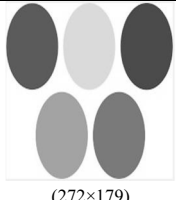
4		7.498	7.490	7.504	7.111	131.6	213.73	191.65	231.12
5		7.526	7.332	7.550	7.384	145.54	322.39	86.3	96.576
6		7.410	6.756	6.112	6.744	176.20	544.69	587.82	403.98
7		7.746	7.575	7.712	7.328	70.27	87.36	69.21	214.61
8		7.142	7.195	7.560	7.445	348.28	259.92	347.34	161.20
9		2.302	3.064	2.228	3.98	112.09	62.063	115.33	60.360

Table 4 (continued)

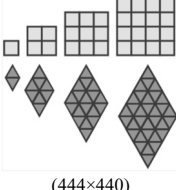
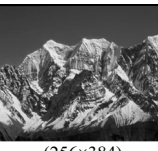
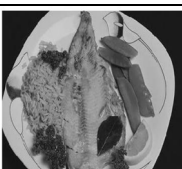
10		6.153	6.899	6.288	5.406	876.29	981.141	314.34	1071.03
11		4.055	1.166	1.915	2.705	188.55	664.840	329.659	379.53
12		7.477	6.781	7.340	7.598	489.321	879.932	612.342	321.567
13		7.156	6.808	7.561	6.865	785.328	1123.67	768.65	904.003
14		7.338	7.714	7.251	4.870	109.123	114.123	238.654	479.128

Table 4 (continued)

15	 (256×384)	7.157	6.508	7.454	6.609	780.56	876.421	502.34	802.45
16	 (256×384)	3.326	5.928	3.143	2.657	256.876	84.234	106.43	333.765
17	 (256×384)	6.931	6.844	7.113	5.950	189.321	234.532	112.98	279.387
18	 (256×384)	2.287	4.811	6.311	5.112	394.312	350.21	278.632	196.543
19	 (256×384)	7.156	5.327	6.951	5.832	286.543	563.218	399.645	542.64
20	 (256×384)	7.190	7.149	7.067	3.906	167.93	186.561	324.654	402.563
21	 (256×384)	3.686	6.587	5.992	5.319	210.32	189.54	113.78	120.543

rotations, are tabulated in Table 4, for all the 21 images. The optimal i.e., minimum entropy values are bold faced. Table 4 depicts the KLD between the original and anamorphic image, for four different rotations, for all the 21 images. The maximum KLD values are bold faced. We can observe that the rotation corresponding to the minimum entropy of the 1/6th portion of the original image matches with the rotation corresponding to the maximum KLD value, for different images. This observation validates the Algorithm 1 which selects the optimal rotation for anamorphic generation. Table 5 depicts the 21 input images, their optimal rotations, and the corresponding anamorphic images. Both Table 4 and Table 5 use $\alpha = 20^\circ$, $d = 1500$, and $h = 546$. The level of distortion available in the proposed optimal anamorphic image generation is compared with the existing high distorted anamorphic image generation proposed by Bobby Stefy et al. [1] and Vesna and Bojan [19]. Bobby Stefy el al. [1] has generated the high distorted anamorphic images with the help of the entropy values and the effect of image rotation is not reported in their work. Therefore, the high distorted anamorphic image is obtained by setting angle, distance, and height as $\alpha = 20^\circ$, $d = 1500$, and $h = 546$. The high distorted anamorphic image suggested by Vesna and Bojan is obtained when the viewing direction is parallel to the picture plane combined with the viewing angle less than 10° and viewing distance closer to the image. Table 6 clearly shows that

Table 5 Anamorphic image generation based on optimal rotation and high KLD value

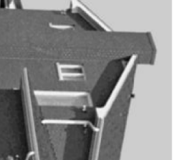
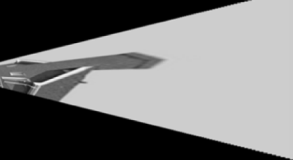
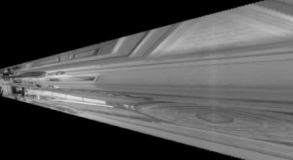
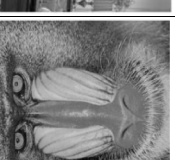
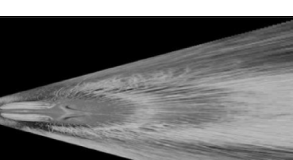
S.No	Input Image	Optimal rotation	Anamorphic image corresponding to optimally rotated image
1			
2			
3			

Table 5 (continued)

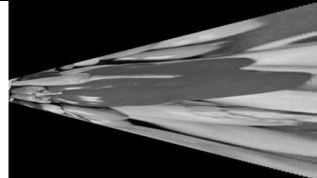
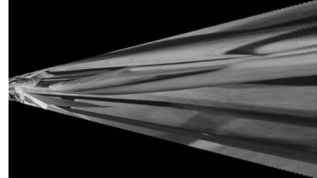
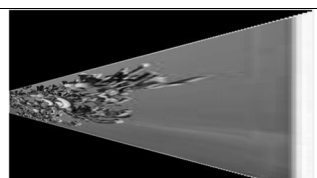
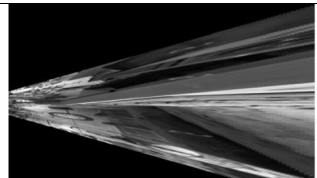
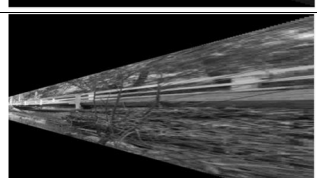
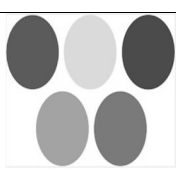
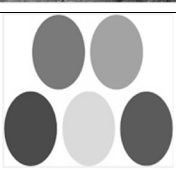
4			
5			
6			
7			
8			
9			

Table 5 (continued)

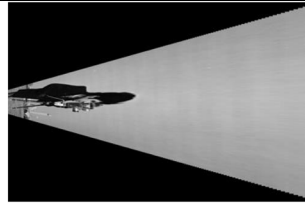
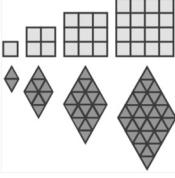
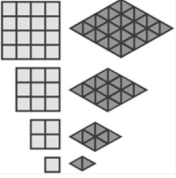
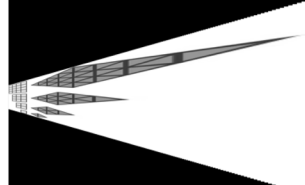
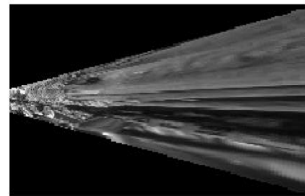
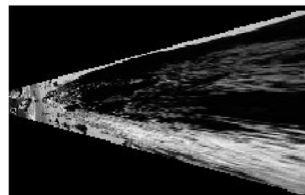
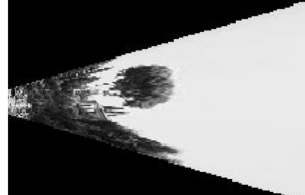
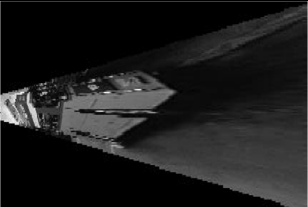
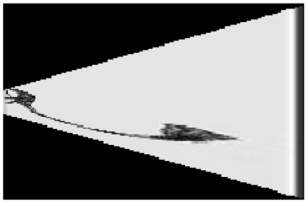
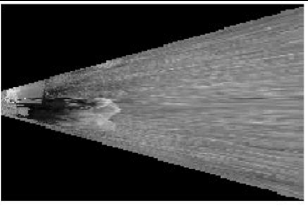
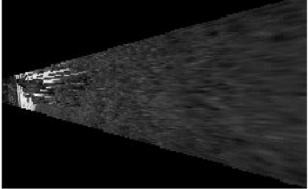
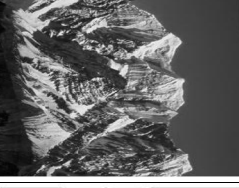
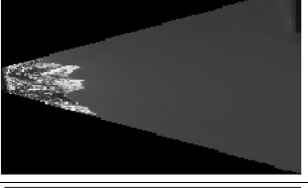
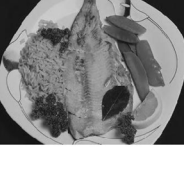
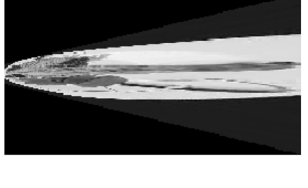
10			
11			
12			
13			
14			

Table 5 (continued)

15			
16			
17			
18			
19			
20			
21			

the optimal rotation of the original image gives more distorted anamorphic image that is evaluated with the help of KLD.

6 Conclusions

The anamorphic models generate the anamorphic images using viewing angle, height, and distance. The impact of viewing point or rotation is not captured in the existing models. The proposed algorithm has a provision to select an optimum rotation of the given image using Shannon's entropy. The algorithm has been verified by applying it on various kinds of images, and the KLD was used to quantify the amount of distortion. The optimum anamorphic generation can be applied to images and videos to encrypt them. Anamorphized images can also be used in steganography. The proposed work is aimed towards planar anamorphosis. This work can be extended to mirror anamorphosis.

Table 6 The proposed method is compared with existing anamorphic image generation methods

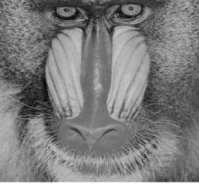
Sl.No	Input Image	Bobby Stefy et al. [11] Rotation=0°	Vesna and Bojan [18] Rotation=0°	Proposed Work KLD+ Optimal Rotation
1		205.75	222.349	KLD= 1086 Optimal Rotation= 270 °
2		89.65	109.345	KLD=379.13 Optimal Rotation= 270 °
3		181.8	203.32	KLD=309.91 Optimal Rotation= 90 °

Table 6 (continued)

4		131.6	158.32	KLD=231.12 Optimal Rotation= 270°
5		145.54	146.345	KLD=322.39 Optimal Rotation= 90°
6		176.20	171.211	KLD=587.82 Optimal Rotation= 180°
7		70.27	71.3	KLD=214.61 Optimal Rotation= 270°
8		348.28	349.32	KLD=348.28 Optimal Rotation= 0°
9		112.09	113.54	KLD=115.33 Optimal Rotation= 180°

Table 6 (continued)

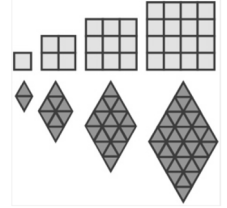
10		876.29	878.43	KLD=1071.03 Optimal Rotation= 270 °
11		188.55	190.432	KLD=664.840 Optimal Rotation= 90 °
12		489.321	490.54	KLD=879.932 Optimal Rotation= 90 °
13		785.328	790.03	KLD=1123.67 Optimal Rotation= 90 °
14		109.123	110.41	KLD=479.128 Optimal Rotation= 270 °
15		780.56	782.65	KLD=876.421 Optimal Rotation= 90 °

Table 6 (continued)

16		256.876	276.43	KLD=333.765 Optimal Rotation= 270°
17		189.321	190.09	KLD=279.387 Optimal Rotation= 270°
18		394.312	395.87	KLD=394.312 Optimal Rotation= 0°
19		286.543	287.54	KLD=563.218 Optimal Rotation= 90°
20		167.93	169.56	KLD=402.263 Optimal Rotation= 270°
21		210.32	209.32	KLD=210.32 Optimal Rotation= 0°

Declarations

Conflict of interest The authors declare that they have no conflict of interest.

References

1. Bobby Stefy Chris S, Pavithra LK, Srinivasan R, Sree Sharmila T (2019) Entropy analysis on planar anamorphic images. *Procedia Computer Science* 165:774–780
2. Bouwers A, Blaisse BS (1956) Anamorphic Mirror Systems. *Journal of SMPTE* 65 (3)
3. Bromiley PA, Thacker NA, Bouhova-Thacker E (2004) Shannon entropy, Renyi entropy, and information, Statistics and Inf. Series
4. Cover T, Thomas J (1991) Elements of information theory. Wiley, New York
5. DeWeerd AJ, Hill SE (2006) Comment on ‘Anamorphic images,’ by J. L. Hunt, B. G. Nickel and Christian Gigault, *Am J Phys.*, 74(1), 83–84, Comment on “Anamorphic images,” by J. L. Hunt, B. G. Nickel, and Christian Gigault [Am. J. Phys. 68(3), 232–237 (2000)]
6. Di Lazzaro P, Murra D, Vitelli P (2019) The interdisciplinary nature of anamorphic images in a journey through art, history and geometry. *Journal of Mathematics and the Arts* 13(4):353–368
7. Di Paola F, Pedone P, Inzerillo L et al (2015) Anamorphic Projection: Analogical/Digital Algorithms. *Nexus Netw* J 17:253. <https://doi.org/10.1007/s00004-014-0225-5>
8. Gonzalez RC, Woods RE (2009) Digital Image Processing. Prentice Hall, 3rd edition
9. Hansford D, Collins D, Tempe AZ (2006) Anamorphic 3D geometry. *Computing* 79:211–223
10. Hu L, Ji Y, Li Y, Gao F (2010) SAR image segmentation based on Kullback-Leibler distance of Edgeworth, advances in multimedia information processing - lecture notes in computer science, vol 6297. Springer, Berlin, Heidelberg
11. Hunt JL, Nickel BG, Gigault C (2000) Anamorphic Image. *Am J Phys* 68(3):232–238
12. Jain A (1986) Fundamentals of digital image processing. prentice-hall
13. Li J, Wang JZ (2003) Automatic linguistic indexing of pictures by a statistical modeling approach. *IEEE Trans Pattern Anal Mach Intell* 25(9):1075–1088
14. Liao X, Yin J, Chen M, Qin Z. Adaptive Payload Distribution in Multiple Images Steganography Based on Image Texture Features, in *IEEE Transactions on Dependable and Secure Computing*. <https://doi.org/10.1109/TDSC.2020.3004708>.
15. Ravnik R, Batagelj B, Kverh B, Solina F (2014) Dynamic Anamorphosis as a Special. Computer-Generated User Interface. *Interacting with Computers* 26(1)
16. Sanchez-Reyes J, Chacon JM (2016) Anamorphic free-form deformation. *Computer Aided Geometric Design* 46:30–42
17. Shapiro A, Todorović D (2017) The Oxford compendium of visual illusions. Oxford University press
18. Singh OP, Singh AK (2021) Data hiding in encryption–compression domain. *Complex & Intelligent Systems*, <https://doi.org/10.1007/s40747-021-00309-w>
19. Stojakovic V, Tepavcevic B (2016) Distortion minimization: a framework for the Design of Plane Geometric Anamorphosis. *Nexus Netw* J 18:759–777. <https://doi.org/10.1007/s00004-016-0302-z>
20. Stork DG (2009) Computer Vision and Computer Graphics Analysis of Paintings and Drawings: An Introduction to the Literature. 13th International Conference on Computer Analysis of Images and Patterns CAIP 2009 Münster, Germany, 2–4
21. Topper D (2000) On anamorphosis: setting some things straight. *Leonardo. JSTOR* 33:115–124
22. Yang B, Zhen-Hong J, Xi-zhong Q, Yang J, Hu Y-j (2013) Remote sensing image enhancement based on relative entropy and fuzzy algorithm. *J Appl Sci* 13:2394–2398

Publisher's note Springer Nature remains neutral with regard to jurisdictional claims in published maps and institutional affiliations.